Environmental Science & Technology

pubs.acs.org/est

Article

Widespread of Potential Pathogen-Derived Extracellular Vesicles Carrying Antibiotic Resistance Genes in Indoor Dust

Yifei Qin, Zihan Guo, Haining Huang, Liting Zhu, Sijun Dong, Yong-Guan Zhu, Li Cui,* and Qiansheng Huang*

Cite This: https://doi.org/10.1021/acs.est.1c08654

Read Online

ACCESS | Metrics & More | Article Recommendations | Supporting Information

ABSTRACT: Extracellular vesicles (EVs) are newly recognized as important vectors for carrying and spreading antibiotic resistance genes (ARGs). However, the ARGs harbored by EVs in ambient environments and the transfer potential are still unclear. In this study, the prevalence of ARGs and mobile genetic elements (MGEs) in EVs and their microbial origins were studied in indoor dust from restaurants, kindergarten, dormitories, and vehicles. The amount of EVs ranged from 3.40×10^7 to 1.09×10^{11} particles/g dust. The length of EV-associated DNA fragments was between 21 bp and 9.7 kb. Metagenomic sequencing showed that a total of 241 antibiotic ARG subtypes encoding resistance to 16 common classes were detected in the EVs from all four fields. Multidrug, quinolone, and macrolide resistance genes were the dominant types. 15 ARG subtypes were exclusively carried and even enriched in EVs compared to the indoor microbiome. Moreover, several ARGs showed co-occurrence with MGEs. The EVs showed distinct taxonomic composition with their original dust microbiota. 30.23% of EV-associated DNA was predicted to originate from potential pathogens. Our results indicated the widespread of EVs carrying ARGs and virulence genes in daily life indoor dust, provided new insights into the status of extracellular DNA, and raised risk concerns on their gene transfer potential.

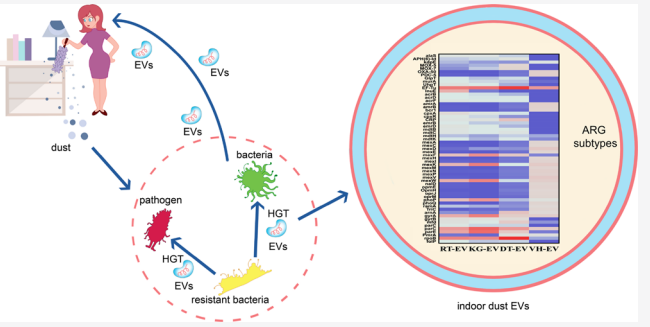

KEYWORDS: *extracellular vesicles, antibiotic resistance genes, indoor dust, mobile genetic elements, pathogen, urban health*

Downloaded via INST OF URBAN ENVIRONMENT on April 19, 2022 at 23:44:10 (UTC).
See https://pubs.acs.org/sharingguidelines for options on how to legitimately share published articles.

1. INTRODUCTION

Antibiotic resistance has been a serious global health threat to the world over the last few decades.[1] Its prevalence, especially in the bacteria of clinical contexts, has compromised antibiotic therapy for pathogen infections greatly.[2] It is estimated that antimicrobial resistance (AMR) infections took 4.95 million lives, including 1.27 million deaths attributable to bacterial AMR in 2019.[3] The spread of antibiotic resistance genes (ARGs) largely accounted for the AMR. ARGs are widely distributed in the environment. Accumulating evidence has revealed that the air environment is a large reservoir of ARGs.[4−6] Airborne transmission has been contempered to be a crucial route for ARGs' spread and exposure.[7,8] Particle matter (PM), which is an important airborne contaminant, offers a large volume of adhering sites, thus enhancing the stability of ARGs in the air.[9] ARGs harbored in PM can be a resource providing antibiotic resistance from the "One Health" perspective.[10] As people spend approximately 90% of their time on indoor activities in modern life,[11] the indoor environment is vital for public health. Therefore, understanding the prevalence, status, and transmission mechanism of ARGs in indoor dust is of great importance for assessing the exposure risk of humans to antibiotic resistance.

In addition to transduction, transformation, and conjugation, which are the three well-characterized routes of the horizontal gene transfer (HGT), extracellular vesicles (EVs) have been proposed to be the fourth approach.[12,13] EVs are spherical and lipid bilayer membrane structures, ranging from 30 to 400 nm in diameter. These nanosized particles can be released by almost all types of microorganisms.[14] EVs have been known to carry and transfer cargoes including lipids, proteins, RNA, and DNA, facilitating communication within cells. Laboratory culture experiments have revealed the roles of EVs in interbacterial ARG transportation. For example, EVs derived from *Acinetobacter baumannii* can deliver plasmid DNA containing carbapenemase genes (e.g., blaOXA-24) to the recipient bacteria, thus transfering beta-lactam antibiotic resistance.[15]

It is exciting to consider that EVs can act as a transfer vector for DNA and other cargoes in the environment. First, EVs can

Received: December 18, 2021
Revised: April 4, 2022
Accepted: April 6, 2022

ACS Publications © XXXX American Chemical Society

protect and prolong the half-life of extracellular DNA. Exporting DNA in a vesicle rather than directly releasing a free-floating DNA molecule into the extracellular milieu can protect DNA from degradation. Second, with a bilayer phospholipid membrane, EVs show high affinity within cells. Third, EVs can form relatively high local concentrations of cargoes. All these can enhance the probability of cargo delivery, such as HGT between cells.

Although several studies have started to focus on the distribution of EVs in the environmental matrices, only one paper looked at the change of ARGs associated with EV-likes particles in the wastewater upon antibiotic treatment.[16] However, currently, studies on the existence of ARGs in EVs and their mediating roles were primarily based on laboratory bacterial culture experiments. The abundance and resistome cargoes of EVs in the air and other in situ environments remain largely unknown, impeding understanding of their ARG transfer roles in the environment. In this work, EVs from the dust of four typical indoor fields were isolated, including restaurants, kindergarten, dormitories, and vehicles. Then, the abundance and diversity of EV-associated DNA, as well as the microbiome from the corresponding field samples, were analyzed using metagenomic sequencing. The objectives of this study were (1) to determine the prevalence of EVs in indoor dust, (2) to elucidate the diversity and abundance of antibiotic resistome in indoor dust-borne EVs, and (3) to reveal the source of EVs in indoor dust. This study provided new insights into the prevalence of ARGs in EVs in daily life indoor dust.

2. METHODS AND MATERIALS

2.1. Sampling of Indoor Dust. Indoor dust was obtained using a vacuum cleaner during the summer of 2020 in Xiamen City, Southeast China. Four types of indoor fields were selected including restaurants, kindergarten, dormitories, and vehicles. For the vehicle sample, dust was collected from vacuum cleaners at seven car wash shops over a month. Dust from the surfaces of floors, shelves, and tables, as well as filters of air conditioners, was harbored from the other three sites. For each sampling field, at least 13 g dust was pooled. The environmental parameters of the sampling sites are listed in Table S1.

2.2. Isolation of EVs from Indoor Dust. Extraction of EVs from the dust samples was processed according to a previous study.[17] Briefly, indoor dust was incubated in phosphate-buffered saline (PBS) in a ratio of 1: 25 (weight: volume) under a rotation speed of 180 rpm for 12 h at 4 °C. A gauze of 75 μm thickness was employed to filter insoluble matters. Bacteria and other large particles were eliminated by centrifugation at 8000 g × 20 min at 4 °C, followed by filtration through 0.45 and 0.22 μm PVDF filters (Millipore) and centrifugation at 10,000 g for 45 min at 4 °C. Then, ultracentrifugation with a Type 41 Ti rotor (Beckman Coulter, USA) at 120,000 × g for 90 min at 4 °C was used to pellet EVs finally. To further remove the contaminating proteins, the pellets were redissolved in PBS and re-centrifuged one more time as above. The prepared indoor dust EVs were stored at −80 °C for further experiments.

2.3. Characterization of EVs from Indoor Dust. Characterization of indoor dust EVs was performed with transmission electron microscopy (TEM) and nano-flow cytometry (nano-FCM). For TEM observation, the EVs were subjected to 4% paraformaldehyde (Sigma-Aldrich) in 0.1 M PBS (pH 7.4), and the solution was placed on a copper mesh. TEM was conducted with a Tecnai G2 Spirit transmission electron microscope (Hitachi, JPN). The size distribution and total particle concentration of EVs were measured by a nano-flow cytometer (N30, NanoFCM, Xiamen, China) according to a previous study.[18] Nano-FCM silica nanosphere cocktail was used as the size reference. The cocktail contained a mixture of silica nanospheres of four different diameters ranging from 68 to 155 nm. The EVs were diluted with PBS to a suitable concentration before analysis, and then three replicates of measurement were performed.

2.4. DNA Extraction. DNA was extracted from EVs and their corresponding dust microbiota using the HiPure soil DNA kit B (Magen, China), following the manufacturers' manual. For indoor dust DNA, the dust samples (2 g) were dissolved in PBS and filtered through a sterile PVDF filter (Millipore). The filter was then subjected to DNA extraction. EV-associated DNA was isolated from the extracted EV samples. The quantity and quality of DNA were determined using a Qubit 3.0 fluorometer (Thermo Fisher, Waltham, USA) and agarose gel electrophoresis, respectively. The extracted DNAs were kept at −20 °C for further use. To be noted, we also studied the interference of the contaminating cellular DNA. In brief, we isolated the EVs from dust and subjected them to DNase (2 U/μL reaction) for 30 min at 37 °C. As a control, another aliquot of EVs was incubated under the same conditions without adding the enzyme. After terminating the incubation, we performed DNA extraction, concentration measurements, and absolute quantification of 16S rRNA genes for both samples (Figure S1). Genomic DNA was used as control to ensure the efficiency of DNase activity.

2.5. Measurement of the Length of EV-Associated DNA Fragments. The length of DNA fragments associated with EVs was analyzed on a 2100 Bioanalyzer (Agilent Technologies, USA) with an Agilent high-sensitivity DNA kit (kit number: 5067-4626), following the manufacturers' manual.

2.6. Absolute Quantification of 16S rRNA Gene. Roche 480 with the SYBR Green method was employed to determine the absolute copy number of the 16S rRNA gene. 10 μL of 2× Light Cycler 480 SYBR Green I Master Mix (Roche Inc., USA), 1 μM of each primer (341 F: 5′-CCTACGGGNGGCWGCAG-3′ and 806 R: 5′-GGAC-TACHVGGGTWTCTAAT-3′), 1 μL of DNA template, and 7 μL of nuclease-free water were used to make a reaction solution of 20 μL. Roche 480 was used for PCR amplification, with an initial preincubation at 95 °C for 5 min, followed by 40 cycles of 95 °C for 15 s, 60 °C for 1 min, and 72 °C for 15 s. A 10-fold dilution of a standard plasmid comprising a cloned and sequenced 16S rRNA gene fragment (1.39×10^{10} copies/L) was used to create an eight-point calibration curve. The PCR reaction was carried out three times in duplicate, including negative and positive controls.

2.7. Metagenomic Analysis. The sequencing library was constructed using a VAHTS Universal DNA Library Prep Kit for Illumina at Genewiz Company in Suzhou, China, following the manufacturer's protocol. A total of 200 ng DNA was used for each sample. End-repair and dA-tailing were performed using the NEBNext Ultra II End-Repair/dA-tailing Module. VAHTSTM DNA Clean Beads were used for purification, and fragments of ~470 bp (with the approximate insert size of 350 bp) were recovered. Then, each sample was amplified by PCR for eight cycles using P5 and P7 primers, with both primers

https://doi.org/10.1021/acs.est.1c08654
Environ. Sci. Technol. XXXX, XXX, XXX−XXX

carrying sequences which can anneal with the flow cell to perform bridge PCR. The P7 primer carries a six-base index allowing for multiplexing. VAHTSTM DNA Clean Beads, Agilent 2100 Bioanalyzer, and Qubit 3.0 fluorometer were employed for cleaning up, validating, and quantifying the PCR products, respectively.

An average of about 66 million clean reads was generated for each DNA sample, resulting in a total of 78.85 Gbps of clean data (Table S2). The software Bcl2fastq (v2.17.1.14) was used to process the raw sequences obtained through Illumina sequencing. Reads with quality score lower than 20 sequences, ambiguous bases (N > 10%), and improper primers were filtered using Cutadapt (v1.9.1) before clustering. The clean data were assembled using MEGAHIT (v1.1.3) with default parameters. Open reading frames (ORFs) from each sample were predicted for the assembled contig set using Prodigal (v2.6.3). The gene sequences of all samples were integrated, and the sequence clustering software CD-HIT (v4.5.6) was used to cluster the genes derived from all samples. A single sequence from each cluster was retained with 95% identity and 90% coverage—this corresponds to one copy of a particular gene per species, which is hereafter referred to as the "unigene". To analyze the relative abundance of unigenes in each sample, paired-end clean reads were mapped to unigenes using SOAPAligner (version 2.2.1) to generate reads' aligned information for unigenes. Gene abundance was calculated based on the number of aligned reads and gene length in each unigene alignment.

2.8. ARG Annotation. Diamond (version v0.8.15.77) was used to search the protein sequences of the nonredundant gene catalog with the Comprehensive Antibiotic Resistance Database (CARD, https://card.mcmaster.ca/),[19,20] with an E-value $<1 \times 10^{-5}$ to explore ARGs. A unigene was annotated as an ARG if the best BLASTP hit showed at least 80% identity over a query coverage of 80%.[21] The identified ARG-like sequence was then manually sorted into various ARG types (e.g., multidrug resistance genes) and subtypes (e.g., mexK) according to CARD. The relative abundances of all ARG sequences from the same type or subtype were calculated to examine the relative abundance of each ARG type and subtype.

2.9. Taxonomic Annotation. For the exploration of the microbial composition, a sequence database of bacteria, fungi, archaea, and viruses from the NR database of NCBI was constructed. The sequences were blasted against the constructed microbial database. MEtaGenome ANalyzer (MEGAN, v6.4.4) was used to determine the lowest common ancestor. The abundance of species in one sample is equal to the sum of the gene abundance annotated for the species. The statistically significant threshold of the sequence alignment was set at 1×10^{-5},[22] and the sequence alignment length was set as no less than 80% of the reference gene-encoding protein length with the identity >80%.[23] The matched result with the best score was selected for annotation.

2.10. MGE Annotation. To explore the diversity and abundance of MGEs, including integrons, insertion sequences (ISs), and plasmid sequence, BLASTN (BLAST Version 2.2.31+) was employed to align the nonredundant gene catalog (for the arrangements of MGEs) against the databases INTEGRALL[24] and Isfinder.[25] We aligned the nonredundant gene catalog to the RefSeq database using BLASTP. Integron or IS sequences were annotated if the best BLASTN (1×10^{-5}) hit had a nucleotide sequence identity no less than 80% over an alignment length >75 bp.[26] A read or contig was determined as a plasmid-like sequence if the best BLASTP (1×10^{-5}) hit showed at least 80% identity.

2.11. Virulence Factor Annotation. VFDB database (http://www.mgc.ac.cn/VFs/) was employed to predict the virulence factor-encoding genes in our study. The virulence factor-encoding genes were annotated if the best BLASTP (E-value 10^{-10}) hit had an amino acid sequence identity higher than 80%.[27]

2.12. Statistical Analysis. Unpaired t tests were conducted using SPSS 25.0 (SPSS, Chicago, USA) after verifying the normality. All statistical tests were considered significant at $p < 0.05$. Principal coordinate analysis (PCoA) based on Bray−Curtis distances and Adonis test was performed by R software (version 4.0.3) with the vegan package 2.2.0.[27]

3. RESULTS

3.1. Existence of EVs in Indoor Dust. To determine the prevalence of EVs in the airborne environment, we isolated EVs in indoor dust collected from four different types of indoor fields. In each field, to make the samples more representative, dust was pooled from multiple sites in multiple spaces. The TEM images showed spherical, homogeneous, and membrane-enclosed structures of EVs (Figure 1a), which were

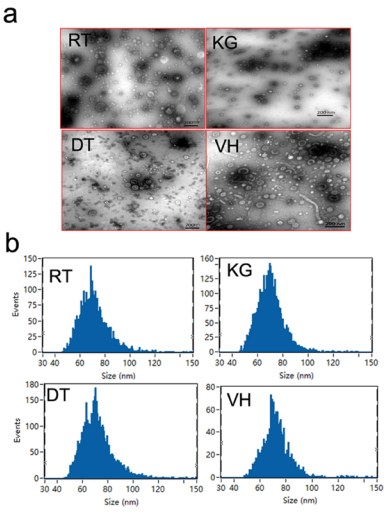

Figure 1. EVs in indoor dust. (a) TEM images of EVs from four fields of indoor dust. Scale bar = 200 nm. (b) Particle size distribution histograms of indoor dust EVs analyzed by nano-FCM analysis. Silica nanosphere cocktails containing four different diameters (68 ± 2, 91 ± 3, 113 ± 3, and 155 ± 3 nm) were used as reference nanoparticles. RT, restaurant; KG, kindergarten; DT, dormitory; VH, vehicle.

similar to those extracted from the culture media of Gram-negative *Escherichia coli* and Gram-positive *Staphylococcus aureus* (Figure S2). The average diameters of EVs from the four sampling fields were very similar, 69.7 ± 11.8 nm in restaurants, 69.9 ± 10.3 nm in kindergarten, 71.7 ± 12.2 nm in dormitories, and 71.2 ± 10.6 nm in vehicles, respectively (Figure 1b). The amount of EVs varied in different fields, ranging from 3.40×10^{7} to 1.09×10^{11} particles/g dust. The concentrations of EVs were similar to or even multiple orders of magnitude higher than that of the number of bacteria determined by the absolute copies of 16S rRNA in the respective fields (Table 1). This showed the wide distribution of EVs together with bacteria across indoor areas. The lengths

https://doi.org/10.1021/acs.est.1c08654
Environ. Sci. Technol. XXXX, XXX, XXX−XXX

Table 1. Size, Concentration, and Double-DNA Concentration of EVs in Indoor Dust

	size nm (mean ± sd)	double-DNA concentration (ng/g)	particle concentration (particles/g)	bacteria concentration (number/g)
RT-EV	69.75 ± 11.28	71.38	3.05×10^{10}	8.88×10^{7}
KG-EV	69.98 ± 10.29	126.02	1.09×10^{11}	1.38×10^{8}
DT-EV	71.71 ± 12.36	4.82	9.17×10^{9}	1.14×10^{9}
VH-EV	71.24 ± 10.62	3.61	3.40×10^{7}	7.05×10^{8}

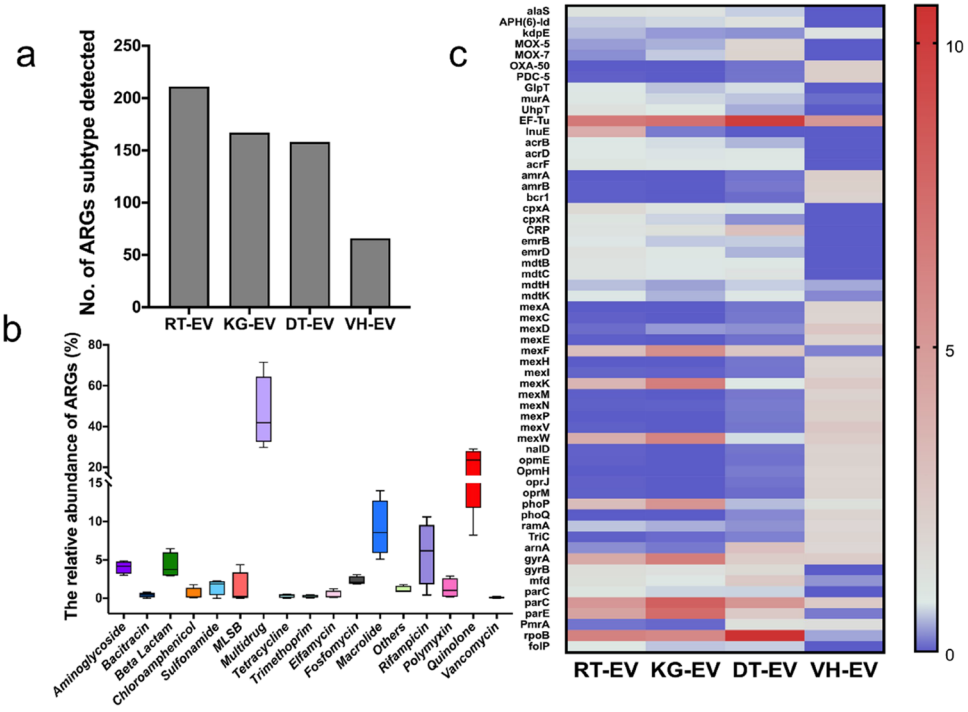

Figure 2. Diversity and abundance of ARGs in indoor dust-borne EVs. (a) Total number of ARG subtypes detected in EVs from indoor dust. (b) Relative abundance of 16 ARG types in EVs from indoor dust. (c) Heatmap of ARG subtypes (relative abundance >1%) in EVs from indoor dust samples.

of EV-associated DNA were in the range from 21 bp to 9.7 kb. Among them, those between 100 bp and 1 kb accounted for the majority (87.34%) (Figure S3 and Table S3).

3.2. Diversity and Abundance of EV-Associated ARGs from Indoor Dust. A metagenomic approach based on CARD was used to profiling the antibiotic resistome of EV-associated DNA. A total of 241 ARG subtypes encoding resistance to 16 common classes of antibiotics were detected. The highest diversity was found in the EVs from restaurants (211), followed by kindergarten (167), dormitories (158), and vehicles (66) (Figure 2a). Twelve out of 16 antibiotic classes were prevalent in all the four field-derived EVs. These indicated that EVs harbored a variety of ARG subtypes. Multidrug (46.27%), quinolone (21.07%), and macrolide (9.05%) resistance genes were the top three dominant types in these samples (Figure 2b). Among the types of mechanisms leading to multidrug resistance, antibiotic efflux accounts for 39.64%, followed by antibiotic target alteration (5.23%), antibiotic target protection (1.26%), and reduced permeability to antibiotics (0.14%). With regard to the 241 ARG subtypes, genes encoding EF-Tu (macrolide), rpoB (rifampicin), and parC (quinolone) were the most prevalent, respectively, with the abundance of 7.27, 5.82, and 5.22%. Notably, 29 ARG subtypes were shared within the four sampling fields (Figure 2c). These data evidenced the high diversity of EV-harboring ARG subtypes in indoor dust.

3.3. Distinct ARG Profiles in EV-Associated DNA Compared to the Genomic DNA of Microbiota. To clarify specific ARG patterns in indoor dust-derived EVs, we compared the ARG profiles between EVs and their original indoor dust microbiota. The ARG profiles in EV-associated DNA differed significantly from that in microbial DNA across all four sampling fields (Adonis test, $p < 0.05$) (Figure S4a). Notably, the number of ARG subtypes detected in EVs (241) was, on average, 28.9% less than that carried by dust (339), indicating that only a subset of microbial ARGs was incorporated into EVs. A total of 29 and 87 ARG subtypes were shared across the four EV populations and the original indoor dust microbiota, respectively. Only 13.72% of the ARG subtypes was shared between EVs and indoor dust. Notably, 15 detected ARG subtypes carried by EVs (14.70%) were absent in dust microbiota (Figure 3a), suggesting that the source of certain EV-associated ARGs may be from nonlocal microbiota. These unique genes in EVs encoded resistance to multidrug (H-NS, TriA, TriC, mdtG, mdtK, mexD, mexI, mexK, mexN, mexW, phoP, and ramA) and quinolone (pmrA, pmrB, and parE) (Figure S4b).

We further compared the relative abundance of ARGs (annotated as ARGs in each sample) between EVs and indoor dust microbiota. ARG subtypes that confer resistance to multidrug or quinolone occupied a relatively high proportion in each EV sample. The average relative abundance of

https://doi.org/10.1021/acs.est.1c08654
Environ. Sci. Technol. XXXX, XXX, XXX−XXX

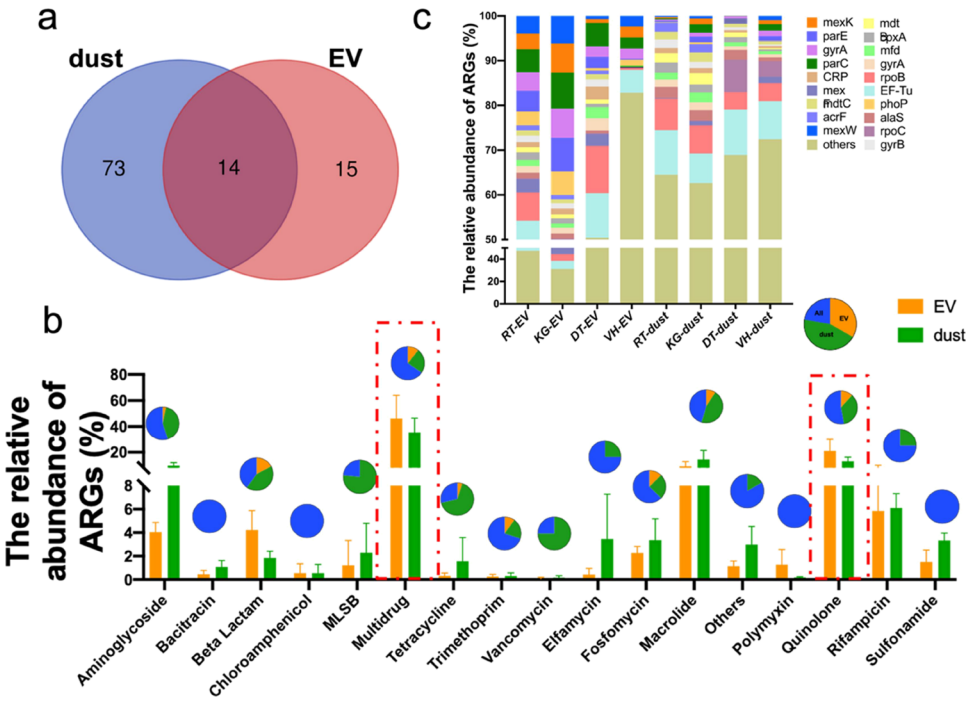

Figure 3. Comparisons of ARG profiles between indoor dust-borne EVs and the microbiota in indoor dust. (a)Venn diagram showing different ARGs in EVs isolated from indoor dust. (b) Comparison of ARGs abundance and diversity (number of ARG subtypes) between EVs and their source indoor dust. The circle plots below indicate the number of ARG subtypes corresponding to this bar. EVs represent the number of genes unique in EVs, dust represents the number of genes unique in dust, and All represents the number of genes co-occurring in both groups. (c) Relative abundance of ARG subtypes in EVs and indoor dust across four fields. The top five abundant types in each group are shown for the respective samples.

multidrug and quinolone was 46.27 and 21.07% in EVs compared to 35.36 and 12.03% in the counterpart dust microbiota (Figure 3b). Within these ARG subtypes, the relative abundance of mexK and mexW conferring multidrug resistance was significantly higher in EVs compared to the microbiota (t test, $p < 0.05$), with the relative abundance ratio of 217.35 and 187.89, respectively. Significant enrichment of ARG subtypes also occurred in quinolone types (t test, $p < 0.05$), in which GyrA, parE, and parC have amplification factors of 5.54, 5.49, and 5.86, respectively (Figure 3c). Moreover, ARGs being selectively enriched in EVs may be another reason for some unique ARGs in EVs. Therefore, the distribution patterns of the antibiotic resistome in EVs are largely distinct to that of the source indoor dust microbiota.

3.4. Mobility of EV-Associated ARGs. In total, 2−8 integrons, 22−26 ISs, and 2560−19,320 plasmid-like sequences were identified in EV-associated DNA (Figure 4a−c). After further classification, we found that intI1 was the most abundant integron type, accounting for 82.70−89.78% of the total integron abundance. Tn3, IS3, and IS5 were the three dominant IS families, totally occupying 46.98−52.51% of the IS abundance (Figure 4d,e). Next, we compared the MGE profiles between EVs and indoor dust microbiota. The number of MGE subtypes is comparable between EVs and dust, especially in integrons and ISs (4−9 integrons, 24−26 ISs, and 16,820−27,741 plasmid-like sequences were detected in dust) (Figure S5a−c). IntI1 is still the most dominant integron type in dust microbiota (67.00−94.42% of the total integron abundance). In contrast, Tn3, which was the most abundant IS type in EVs, only accounted for about 3% in dust (Figure S5d,e). A total of 2566 co-occurring contigs were found. The length range of these contigs was between 153 and 4029 bp, and over 75% of contigs were between 400 and 1000 bp in length. The distribution of sequence lengths is listed in Figure S6. ISL3 was the only IS type co-occurring with the ARGs in EVs from restaurants and kindergarten. Further, the type of ARG that ISL3 carried was multidrug (Figure 4f). In contrast, there was no ARG−MGE cluster detected in dormitories and vehicles. IntI1 was the only integron type that co-occurred with ARGs in all four samples except vehicles. Aminoglycoside and beta-lactam were the two most dominant types of ARGs co-occurring with IntI1, accounting for 73.24−83.02% (Figure 4g). We also observed several plasmid-like sequences co-occurring with ARGs, mainly consisting of multidrug, quinolone, and macrolide (Figure 4h). Examples of the arrangement of ARG−MGE clusters in the EVs are shown in Figure S7. Compared to EVs, ARG−MGE clusters were detected in all the dust microbiota samples. In addition to ISL3, both IS1595 and IS481 in the microbiota also co-occurred with some ARGs (Table S4). IntI1 was still the only integron type that co-occurred with ARGs in all four dust samples. It mostly co-occurred with aminoglycoside instead of aminoglycoside and beta-lactam compared to IntI1 from vesicles (Figure S5f). Similar to the EV group, the top three ARG classes that co-occurred with plasmid-like sequences are multidrug, macrolide, and quinolone in dust samples (Figure S5g).

3.5. Enrichment of EVs Derived from Antibiotic-Resistant Pathogenic Species. Compared to the taxonomic profiles of the indoor dust microbiota sample, EV-associated DNA showed less microbial diversity (Figure S8). The microbial composition which produced EVs in all four fields differed significantly from that of the surrounding indoor dust (Adonis, $p < 0.01$) (Figure 5a). At the species level, the top five

https://doi.org/10.1021/acs.est.1c08654
Environ. Sci. Technol. XXXX, XXX, XXX−XXX

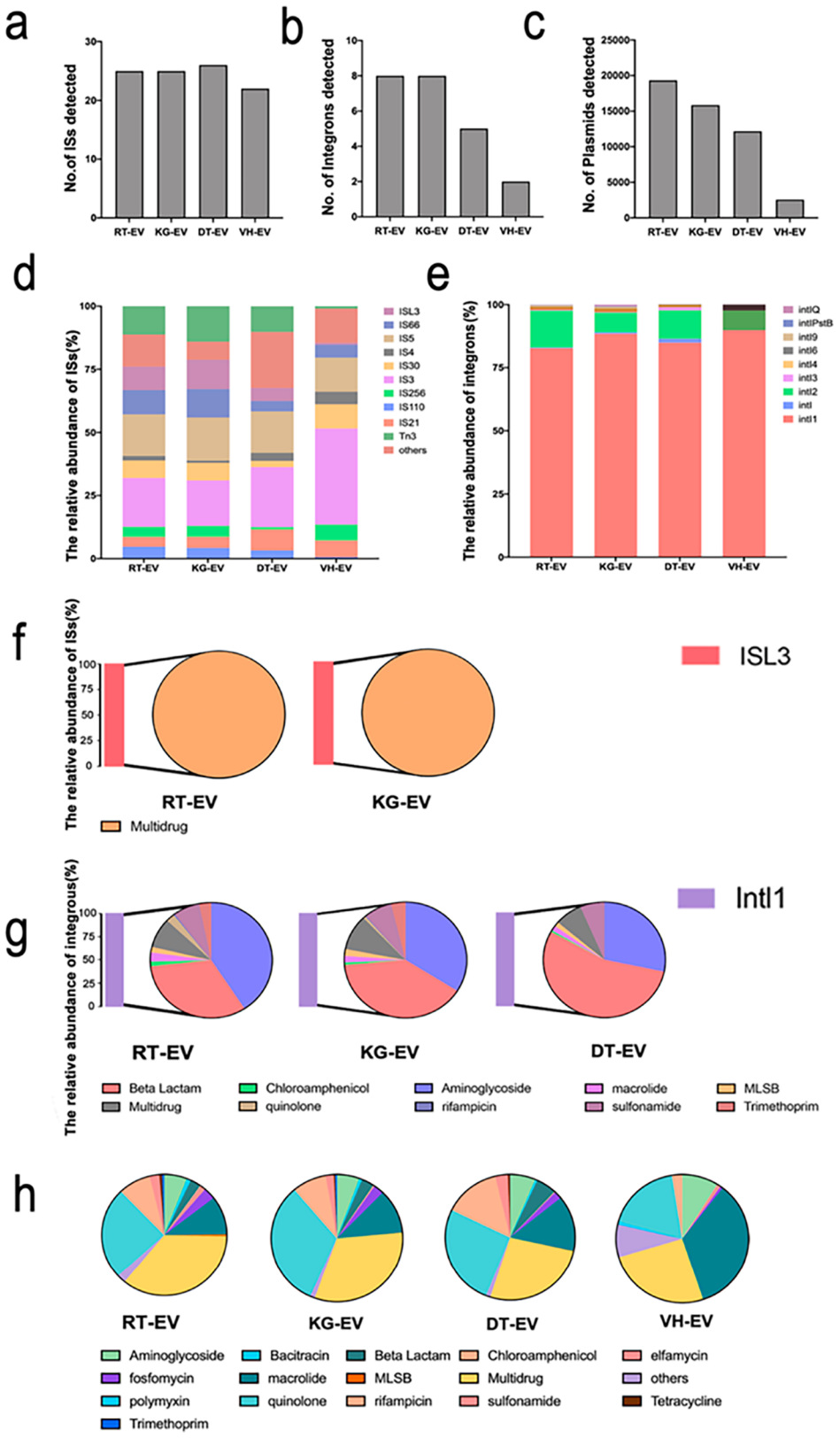

Figure 4. Distribution of mobile genetic elements in indoor dust-borne EVs. (a−c) Number of ISs, integrons, and plasmids. (d) Relative abundance of varied types of ISs classified by family name. (e) Relative abundance of varied types of integrons classified by gene name. (f) Relative abundance of ARG types carried by ISs. (g) Relative abundance of ARG types carried by integrons. (h) Relative abundance of ARG types carried by plasmids.

in EVs were dominated by *Pseudomonas aeruginosa* (11.46%), *P. putida* (7.82%), *Aeromonas caviae* (3.95%), *Enterobacter hormaechei* (1.08%), and *Vibrio fluvialis* (0.98%) (Figure 5c). By contrast, the top five species in dust microbiota were *Klebsiella pneumoniae* (3.52%), *P. stutzeri* (2.29%), *Bacillus megaterium* (1.79%), *E. cloacae* (1.62%), and *V. fluvialis*

https://doi.org/10.1021/acs.est.1c08654
Environ. Sci. Technol. XXXX, XXX, XXX−XXX

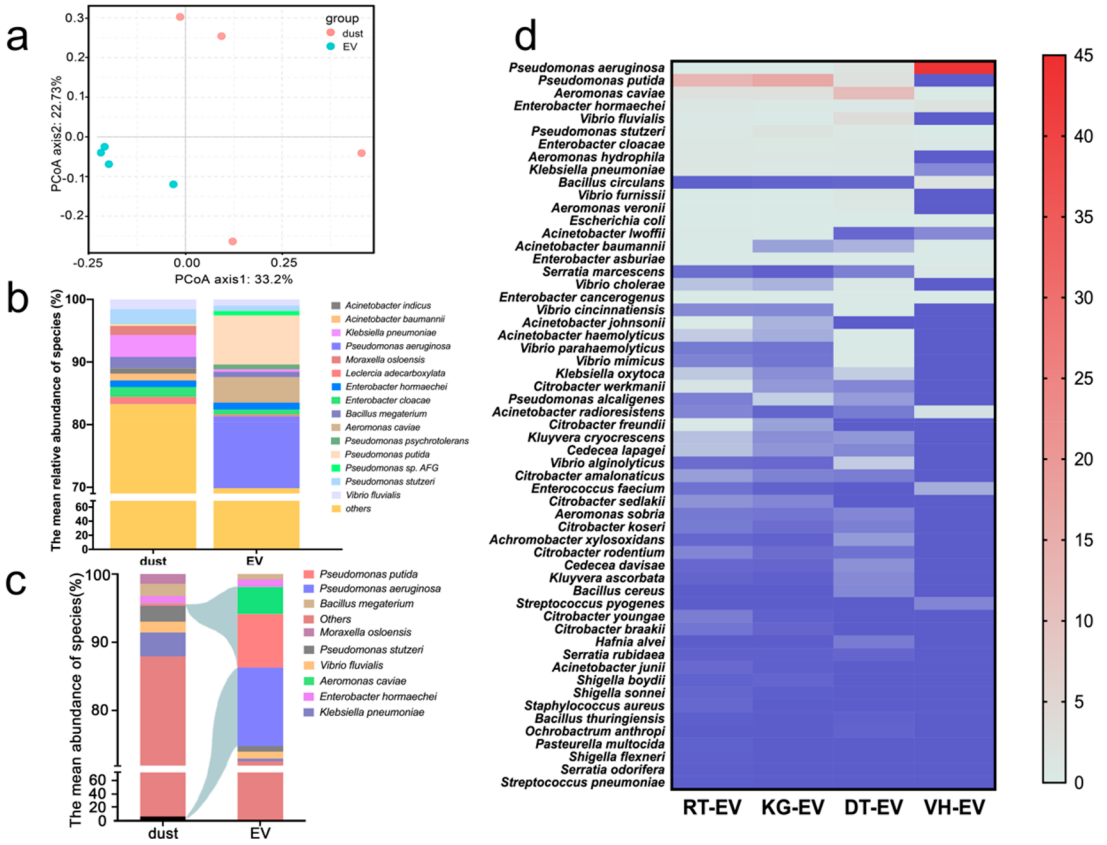

Figure 5. Taxonomic profiles of microbial communities in indoor dust-borne EVs and the microbiota in indoor dust. (a) PCoA based on Bray–Curtis distances showing the patterns of microbial communities (Adonis, $P < 0.001$). (b) Dominant species present in EVs and surrounding indoor dust (top 10 in each group). (c) Sankey diagram shows that rare taxa make a large contribution to the secretion of EVs (top 10 in each group). (d) Heatmap of the pathogen species types and the relative abundances predicted in EVs.

(1.56%) (Figure 5b). Further comparison of the microbial community showed that rare taxa (relative abundance <1%) made a huge contribution to the EV population (Figure 5c). For example, the relative abundance of *P. putida* in EVs was 7.82%, whereas that in the dust was 0.32%. We also detected *A. caviae* in EVs with the relative abundance of 3.95% compared to 0.04% in indoor dust samples. These results demonstrated the distinct taxonomic composition between EVs and the original indoor dust microbiota.

To detect the potential pathogen composition in EV taxa, the species-level taxonomic list was further compared with the pathogen list proposed in a previous study.[28] Approximately 6.41% of all species were identified to be potential pathogens affiliated to 57 bacterial pathogenic species (Figure 5d). Remarkably, EVs possessed a higher pathogen abundance, with the total average relative abundance of 30.23% compared to that of 17.38% in dust. Using VFDB as the reference, a total of 342 virulence factors were predicted in EV-associated DNA, including pyoverdine, lipo-oligosaccharide, lipopolysaccharide, and fbpABC (Table S5). Together, dust EVs can be a reservoir of virulence genes from pathogens.

The pathogenic host of EV-associated ARG subtypes was further determined. A total of 10 potential pathogenic bacteria species ranking top five in each sample are presented in Figure 6a. All the identified potential pathogenic bacteria species primarily belonged to the Gammaproteobacteria class (99.62%), including *Aeromonas*, *Acinetobacter*, *Escherichia*, *Enterobacter*, *Klebsiella*, *Pseudomonas*, and *Serratia*. Among them, Enterobacter was the most abundant genus, accounting for 41.76%. Remarkably, four species in the panel of pathogens, *E. cloacae* (21.62%), *E. hormaechei* (20.07%), *E. coli* (5.53%), and *K. pneumoniae* (2.51%), harbored a high diversity of ARGs (at least eight types). Further, the most abundant ARGs carried by these potential pathogens were those conferring multidrug and quinolone resistance, accounting for 63.01% of the total detected ARG subtypes (Figure 6b). The presence of these potential pathogens was further investigated. Six species (*A.baumannii*, *Serratia marcescens*, *P. aeruginosa*, *E. cloacae*, *E. coli*, and *K. pneumoniae*) were found across all four EV populations (Figure 6c). Furthermore, contigs which were defined as ARG–MGE clusters were also found in EVs' potential pathogenic hosts (Table S6).

4. DISCUSSION

4.1. EVs Are Prevalent in Daily Indoor Dust. The existence of EVs in the environmental media is receiving great attention. EVs were found in indoor dust.[17,29] For other types of environmental matrix, the concentration of EVs ($\sim 10^5$–10^6 vesicles mL^{-1}) comparable to that of bacterial cells was reported in open ocean sea water.[30] EVs formed the components of wastewater effluent as well, with the levels at 2×10^6 mL^{-1}.[16] In this study, we demonstrated the high abundance of EVs existed in all four fields of indoor dust. Comparable amounts or even multiple orders of magnitude more abundant of EVs than bacterial cells in the same site indicated the prevalence of EVs in indoor dust environment. To be noted, the particle concentration could be overestimated in the EV samples extracted from ultracentrifuguation.[18] Our

https://doi.org/10.1021/acs.est.1c08654
Environ. Sci. Technol. XXXX, XXX, XXX–XXX

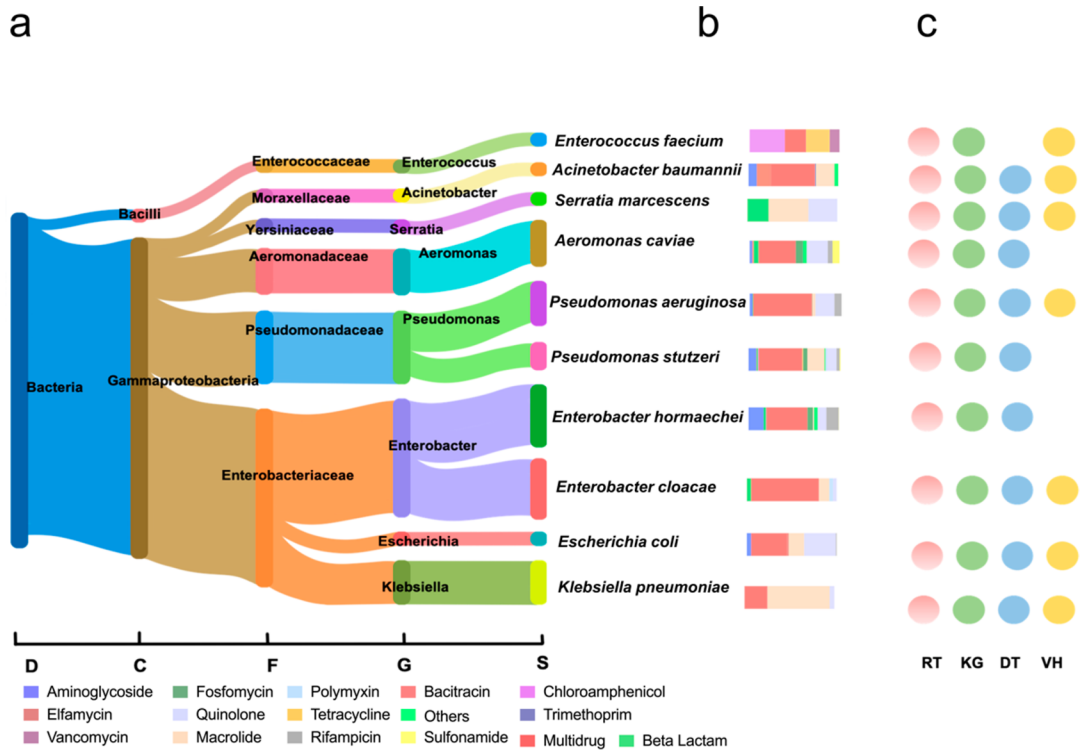

Figure 6. Pathogenic host range of EV-associated ARGs. (a) Composition and relative abundance of the EV-associated ARG hosts (the top five species in each group are shown). (b) Diversity and relative abundance of the ARGs (18 types) carried by the corresponding potential pathogens. The ARG types are colored as indicated in the figure. (c) Distribution of the pathogen hosts of ARGs across four sampling fields. The existence is indicated by the presence of color balls.

work further expanded the sampling range of dust covering various fields of indoor daily life and found that EVs are ubiquitous in varied indoor airborne environments, highlighting the close contact with our body. Moreover, as a dry and nutrition-poor atmosphere, the abundance of EVs in indoor dust extended our understanding on the existence scope of EVs. Combined with previous studies, we conclude that EVs are abundant in a variety of environments, raising the importance of further studies about their cargo and roles in the environment.[14]

4.2. EVs Act as Reservoirs of ARGs. We found that the dust EVs carried a wide array of DNA fragments. The length of EV-associated DNA was heterogeneous, with the range between 21 and 9.7 kb. Diverse lengths were also found in EV-associated DNA from seawater.[31] This length range was enough to encode multiple genes. We did predict diverse EV-associated ARGs with a total of 241 subtypes. A number of ARGs are often located on MGEs to facilitate the spread between various bacterial species.[32,33] We also found different types of MGEs in EV samples. Moreover, multiple ARG−MGE clusters were predicted, indicating the high spread probability of ARGs carried by EVs. These findings provide new insights into the transfer risk of antibiotic resistome via EVs in the field.

Previous studies have reported the distribution of ARGs in dust and ambient environments.[6,34,35] As DNA fragments, ARGs can stay inside the bacteria as genomic or plasmid DNA. They can also stay outside the bacteria, as free extracellular DNA or bound to particles. Our study provided a new layer of the existing form of ARGs in EVs. As lipid bilayer vesicles, EVs can protect their cargoes from degradation by extracellular degrading enzymes. The prolonged extracellular DNA in the environment can thus enhance the probability of HGT events upon successful interactions with new host cells. In addition, EVs can also favor gene transfer by concentrating relatively high local DNA concentrations. The low barrier within bacteria due to the lipid membrane is another advantage. Packing with EVs could provide ARGs a possible transfer route in the environment.

Significant differences in abundance were observed in specific ARGs between EVs and dust microbiota (t test, $p < 0.05$). EVs showed notable enrichment of ARGs to multidrug and quinolone compared to their original dust microbiome. Specific genes, such as gyrA, parE, parC, mexK, and mexW were detected at a high level in EVs but almost below the detection limit in indoor dust. Our results demonstrated that EVs do not simply mimic cellular ARGs but can be specifically enriched or depleted in some components. This indicates that the low abundance of ARGs among indoor dust bacteria cannot be ignored, as they could be selectively encapsulated by EVs and potentially spread within the microbial community.

4.3. Distinct Taxonomic Composition of EV-Associated DNA and Cellular DNA from the Source Dust Microbiome. We performed the metagenomic analysis of DNA from indoor dust microbiota and the derived EVs to figure out the potential origin of EVs. The diversity of taxonomic composition on EV-associated DNA was less than that of the habitat microbial genomic DNA. This implied that in the real environment, the release of EVs was largely influenced by environmental conditions, including, but not limited to, nutrition and environmental stress. Relatively poor growth conditions might restrain the generation and release of EVs by indoor dust microbes. However, active secretion from the bacteria in dust might not be the only source of EV production. Cell lysis, which occurred as a natural process in

https://doi.org/10.1021/acs.est.1c08654
Environ. Sci. Technol. XXXX, XXX, XXX−XXX

dust, could be another way of EV generation in dust.[14] In addition, as EVs possess high stability,[36,37] they could be transported from nonlocal bacteria over long distances in air. We do not rule out the possibility that EVs may be from potential human pathogens or enteric microbes and be "picked up" by the dust particles.

EVs have been shown to act as mediators during the pathological process between the pathogen and its host. It elicited inflammation, immune evasion, and finally the pathology of various infective diseases. For example, EVs from Bacteroides and Prevotella, which are the commensal microbes in lungs, induced the expression of interleukin-17β and promoted the pathogenesis of pulmonary fibrosis.[38] EVs secreted by *Neisseria gonorrhoeae*, uropathogenic *E.coli*, and *P. aeruginosa* induced immune responses in macrophages.[39] EVs spread in indoor dust can enter the respiratory system through inhalation, thus posing a potential health risk. One study showed that indoor dust EVs from a dormitory building, mainly from Pseudomonas, can enhance melanoma lung metastasis in a dose-dependent manner in mice.[17] Further, pathogen-derived EVs were abundantly found in body fluids and tissue biopsies of human patients in vivo studies.[40−42] In our study, a total of 57 potential pathogens were identified as potential hosts of indoor EVs. Their relative abundance in EV taxa was significantly higher than that in the microbiome of indoor dust. As EVs have been shown to be an effective factor for the virulence of *Pseudomonas*, the threat should be concerned even though *Pseudomonas* is a "rare species" in the microbial community of dust. Furthermore, these pathogen-secreted EVs also harbored virulence factor-encoding genes and ARGs, which could exacerbate the potential health risk via the transfer of antibiotic resistance.

To be noted, the lack of DNase treatment to the EV samples prior to DNA extraction means that our analysis may include some contaminating cellular DNA, which might be co-pelleted in the sample. Further works related to EVs in the environmental milieu need to consider the influence of extracellular DNA, especially in cellular DNA-abundant fields, such as sewage.

In summary, the study presented the diverse taxonomic composition of EVs in indoor dust from various daily life fields. A higher relative abundance of pathogen-derived EVs was found compared to the original dust microbiota. Indoor dust EVs harbored a diversity of ARGs. ARGs encoding resistance to multidrug, quinolone, and macrolide coexisting with MGEs were carried by EVs. The reservoir roles of EVs for airborne ARGs extend our knowledge of the existing form of extracellular DNA in dust. Considering the long persistence, protection, local concentration, and mediation roles of EVs on their cargoes, the spread of ARGs and their transfer risk on antibiotic resistance via EVs in the indoor environment are worth more attention from the "One Health" perspective. Future studies are warranted to assess the risk of threat from the urban airborne transmission of ARGs.

■ ASSOCIATED CONTENT

Supporting Information

The Supporting Information is available free of charge at https://pubs.acs.org/doi/10.1021/acs.est.1c08654.

Sampling information; metagenomics data statistics; size range of EV-DNA fragments; virulence factors associated with EVs; ARG−MGE clusters associated with EVs; DNA concentration of EVs with +/− DNase; TEM of bacterial EVs; PCoA analysis of EVs and dust; MGEs in dust; and microbial diversity of EVs and dust (PDF)

■ AUTHOR INFORMATION

Corresponding Authors

Li Cui − *Xiamen Key Laboratory of Indoor Air and Health, Key Lab of Urban Environment and Health, Institute of Urban Environment, Chinese Academy of Sciences, Xiamen 361021, China;* orcid.org/0000-0002-0708-8899; Phone: +86-592-6190780; Email: lcui@iue.ac.cn

Qiansheng Huang − *Xiamen Key Laboratory of Indoor Air and Health, Key Lab of Urban Environment and Health, Institute of Urban Environment, Chinese Academy of Sciences, Xiamen 361021, China; National Basic Science Data Center, Beijing 100190, China;* orcid.org/0000-0002-3788-3164; Phone: +86-592-6190542; Email: qshuang@iue.ac.cn

Authors

Yifei Qin − *Xiamen Key Laboratory of Indoor Air and Health, Key Lab of Urban Environment and Health, Institute of Urban Environment, Chinese Academy of Sciences, Xiamen 361021, China; College of Resources and Environment, University of Chinese Academy of Sciences, Beijing 100049, China*

Zihan Guo − *Institute of Life Science and Green Development, Hebei University, Baoding 071002, China*

Haining Huang − *Xiamen Key Laboratory of Indoor Air and Health, Key Lab of Urban Environment and Health, Institute of Urban Environment, Chinese Academy of Sciences, Xiamen 361021, China*

Liting Zhu − *Xiamen Key Laboratory of Indoor Air and Health, Key Lab of Urban Environment and Health, Institute of Urban Environment, Chinese Academy of Sciences, Xiamen 361021, China; College of Resources and Environment, University of Chinese Academy of Sciences, Beijing 100049, China*

Sijun Dong − *Institute of Life Science and Green Development, Hebei University, Baoding 071002, China*

Yong-Guan Zhu − *Xiamen Key Laboratory of Indoor Air and Health, Key Lab of Urban Environment and Health, Institute of Urban Environment, Chinese Academy of Sciences, Xiamen 361021, China;* orcid.org/0000-0003-3861-8482

Complete contact information is available at: https://pubs.acs.org/10.1021/acs.est.1c08654

Author Contributions

Y.Q., Q.H., and L.C. prepared the manuscript and conducted data analysis. Z.G., L.Z., and H.H. contributed to sample collection. Y.Q. and H.H. performed the experiment. Y.-G.Z. and S.D. helped perform the analysis with constructive discussions. All co-authors provided intellectual and substantive contributions to the manuscript.

Notes

The authors declare no competing financial interest.
https://datapid.cn/31253.11.sciencedb.01159.

■ ACKNOWLEDGMENTS

This study was supported by the National Key R&D Program of China (2018YFE0103300), the National Natural Science Foundation of China (32161143016, 42177362), Fujian

Provincial Department of Science and Technology (2021J06037), National Basic Science Data Center "Environment Health DataBase" (NO.NBSDC-DB-21).

REFERENCES

(1) Zhu, Y. G.; Zhao, Y.; Li, B.; Huang, C. L.; Zhang, S. Y.; Yu, S.; Chen, Y. S.; Zhang, T.; Gillings, M. R.; Su, J. Q. Continental-scale pollution of estuaries with antibiotic resistance genes. *Nat. Microbiol.* **2017**, *2*, 16270.

(2) Walsh, C. Molecular mechanisms that confer antibacterial drug resistance. *Nature* **2000**, *406*, 775−781.

(3) Murray, C. J. L.; Ikuta, K. S.; Sharara, F.; Swetschinski, L.; Robles Aguilar, G.; Gray, A.; Han, C.; Bisignano, C.; Rao, P.; Wool, E.; Johnson, S. C.; Browne, A. J.; Chipeta, M. G.; Fell, F.; Hackett, S.; Haines-Woodhouse, G.; Kashef Hamadani, B. H.; Kumaran, E. A. P.; McManigal, B.; Agarwal, R.; Akech, S.; Albertson, S.; Amuasi, J.; Andrews, J.; Aravkin, A.; Ashley, E.; Bailey, F.; Baker, S.; Basnyat, B.; Bekker, A.; Bender, R.; Bethou, A.; Bielicki, J.; Boonkasidecha, S.; Bukosia, J.; Carvalheiro, C.; Castañeda-Orjuela, C.; Chansamouth, V.; Chaurasia, S.; Chiurchiù, S.; Chowdhury, F.; Cook, A. J.; Cooper, B.; Cressey, T. R.; Criollo-Mora, E.; Cunningham, M.; Darboe, S.; Day, N. P. J.; de Luca, M.; Dokova, K.; Dramowski, A.; Dunachie, S. J.; Eckmanns, T.; Eibach, D.; Emami, A.; Feasey, N.; Fisher-Pearson, N.; Forrest, K.; Garrett, D.; Gastmeier, P.; Giref, A. Z.; Greer, R. C.; Gupta, V.; Haller, S.; Haselbeck, A.; Hay, S. I.; Holm, M.; Hopkins, S.; Iregbu, K. C.; Jacobs, J.; Jarovsky, D.; Javanmardi, F.; Khorana, M.; Kissoon, N.; Kobeissi, E.; Kostyanev, T.; Krapp, F.; Krumkamp, R.; Kumar, A.; Kyu, H. H.; Lim, C.; Limmathurotsakul, D.; Loftus, M. J.; Lunn, M.; Ma, J.; Mturi, N.; Munera-Huertas, T.; Musicha, P.; Mussi-Pinhata, M. M.; Nakamura, T.; Nanavati, R.; Nangia, S.; Newton, P.; Ngoun, C.; Novotney, A.; Nwakanma, D.; Obiero, C. W.; Olivas-Martinez, A.; Olliaro, P.; Ooko, E.; Ortiz-Brizuela, E.; Peleg, A. Y.; Perrone, C.; Plakkal, N.; Ponce-de-Leon, A.; Raad, M.; Ramdin, T.; Riddell, A.; Roberts, T.; Robotham, J. V.; Roca, A.; Rudd, K. E.; Russell, N.; Schnall, J.; Scott, J. A. G.; Shivamallappa, M.; Sifuentes-Osornio, J.; Steenkeste, N.; Stewardson, A. J.; Stoeva, T.; Tasak, N.; Thaiprakong, A.; Thwaites, G.; Turner, C.; Turner, P.; van Doorn, H. R.; Velaphi, S.; Vongpradith, A.; Vu, H.; Walsh, T.; Waner, S.; Wangrangsimakul, T.; Wozniak, T.; Zheng, P.; Sartorius, B.; Lopez, A. D.; Stergachis, A.; Moore, C.; Dolecek, C.; Naghavi, M. Global burden of bacterial antimicrobial resistance in 2019: a systematic analysis. *Lancet* **2022**, *399*, 629−655.

(4) Ben Maamar, S.; Glawe, A. J.; Brown, T. K.; Hellgeth, N.; Hu, J.; Wang, J. P.; Huttenhower, C.; Hartmann, E. M. Mobilizable antibiotic resistance genes are present in dust microbial communities. *PLoS Pathog.* **2020**, *16*, No. e1008211.

(5) Gat, D.; Mazar, Y.; Cytryn, E.; Rudich, Y. Origin-Dependent Variations in the Atmospheric Microbiome Community in Eastern Mediterranean Dust Storms. *Environ. Sci. Technol.* **2017**, *51*, 6709−6718.

(6) Li, J.; Cao, J.; Zhu, Y. G.; Chen, Q. L.; Shen, F.; Wu, Y.; Xu, S.; Fan, H.; Da, G.; Huang, R. J.; Wang, J.; de Jesus, A. L.; Morawska, L.; Chan, C. K.; Peccia, J.; Yao, M. Global Survey of Antibiotic Resistance Genes in Air. *Environ. Sci. Technol.* **2018**, *52*, 10975−10984.

(7) Gao, M.; Qiu, T.; Sun, Y.; Wang, X. The abundance and diversity of antibiotic resistance genes in the atmospheric environment of composting plants. *Environ. Int.* **2018**, *116*, 229−238.

(8) Smillie, C. S.; Smith, M. B.; Friedman, J.; Cordero, O. X.; David, L. A.; Alm, E. J. Ecology drives a global network of gene exchange connecting the human microbiome. *Nature* **2011**, *480*, 241−244.

(9) Hu, J.; Zhao, F.; Zhang, X. X.; Li, K.; Li, C.; Ye, L.; Li, M. Metagenomic profiling of ARGs in airborne particulate matters during a severe smog event. *Sci. Total Environ.* **2018**, *615*, 1332−1340.

(10) Wu, D.; Jin, L.; Xie, J.; Liu, H.; Zhao, J.; Ye, D.; Li, X. D. Inhalable antibiotic resistomes emitted from hospitals: metagenomic insights into bacterial hosts, clinical relevance, and environmental risks. *Microbiome* **2022**, *10*, 19.

(11) Klepeis, N. E.; Nelson, W. C.; Ott, W. R.; Robinson, J. P.; Tsang, A. M.; Switzer, P.; Behar, J. V.; Hern, S. C.; Engelmann, W. H. The National Human Activity Pattern Survey (NHAPS): a resource for assessing exposure to environmental pollutants. *J. Exposure Anal. Environ. Epidemiol.* **2001**, *11*, 231−252.

(12) Domingues, S.; Nielsen, K. M. Membrane vesicles and horizontal gene transfer in prokaryotes. *Curr. Opin. Microbiol.* **2017**, *38*, 16−21.

(13) Soler, N.; Forterre, P. Vesiduction: the fourth way of HGT. *Environ. Microbiol.* **2020**, *22*, 2457−2460.

(14) Toyofuku, M.; Nomura, N.; Eberl, L. Types and origins of bacterial membrane vesicles. *Nat. Rev. Microbiol.* **2019**, *17*, 13−24.

(15) Rumbo, C.; Fernández-Moreira, E.; Merino, M.; Poza, M.; Mendez, J. A.; Soares, N. C.; Mosquera, A.; Chaves, F.; Bou, G. Horizontal transfer of the OXA-24 carbapenemase gene via outer membrane vesicles: a new mechanism of dissemination of carbapenem resistance genes in Acinetobacter baumannii. *Antimicrob. Agents Chemother.* **2011**, *55*, 3084−3090.

(16) Maestre-Carballa, L.; Lluesma Gomez, M.; Angla Navarro, A.; Garcia-Heredia, I.; Martinez-Hernandez, F.; Martinez-Garcia, M. Insights into the antibiotic resistance dissemination in a wastewater effluent microbiome: bacteria, viruses and vesicles matter. *Environ. Microbiol.* **2019**, *21*, 4582−4596.

(17) Dinh, N. T. H.; Lee, J.; Lee, J.; Kim, S. S.; Go, G.; Bae, S.; Jun, Y. I.; Yoon, Y. J.; Roh, T. Y.; Gho, Y. S. Indoor dust extracellular vesicles promote cancer lung metastasis by inducing tumour necrosis factor-alpha. *J. Extracell. Vesicles* **2020**, *9*, No. 1766821.

(18) Tian, Y.; Gong, M.; Hu, Y.; Liu, H.; Zhang, W.; Zhang, M.; Hu, X.; Aubert, D.; Zhu, S.; Wu, L.; Yan, X. Quality and efficiency assessment of six extracellular vesicle isolation methods by nano-flow cytometry. *J. Extracell. Vesicles* **2020**, *9*, No. 1697028.

(19) Alcock, B. P.; Raphenya, A. R.; Lau, T. T. Y.; Tsang, K. K.; Bouchard, M.; Edalatmand, A.; Huynh, W.; Nguyen, A. V.; Cheng, A. A.; Liu, S.; Min, S. Y.; Miroshnichenko, A.; Tran, H. K.; Werfalli, R. E.; Nasir, J. A.; Oloni, M.; Speicher, D. J.; Florescu, A.; Singh, B.; Faltyn, M.; Hernandez-Koutoucheva, A.; Sharma, A. N.; Bordeleau, E.; Pawlowski, A. C.; Zubyk, H. L.; Dooley, D.; Griffiths, E.; Maguire, F.; Winsor, G. L.; Beiko, R. G.; Brinkman, F. S. L.; Hsiao, W. W. L.; Domselaar, G. V.; McArthur, A. G. CARD 2020: antibiotic resistome surveillance with the comprehensive antibiotic resistance database. *Nucleic Acids Res.* **2019**, *48*, D517−D525.

(20) McArthur, A. G.; Waglechner, N.; Nizam, F.; Yan, A.; Azad, M. A.; Baylay, A. J.; Bhullar, K.; Canova, M. J.; de Pascale, G.; Ejim, L.; Kalan, L.; King, A. M.; Koteva, K.; Morar, M.; Mulvey, M. R.; O'Brien, J. S.; Pawlowski, A. C.; Piddock, L. J.; Spanogiannopoulos, P.; Sutherland, A. D.; Tang, I.; Taylor, P. L.; Thaker, M.; Wang, W.; Yan, M.; Yu, T.; Wright, G. D. The comprehensive antibiotic resistance database. *Antimicrob. Agents Chemother.* **2013**, *57*, 3348−3357.

(21) Gibson, M. K.; Forsberg, K. J.; Dantas, G. Improved annotation of antibiotic resistance determinants reveals microbial resistomes cluster by ecology. *ISME J.* **2015**, *9*, 207−216.

(22) MetaHIT Consortium; Qin, J.; Li, R.; Raes, J.; Arumugam, M.; Burgdorf, K. S.; Manichanh, C.; Nielsen, T.; Pons, N.; Levenez, F.; Yamada, T.; Mende, D. R.; Li, J.; Xu, J.; Li, D.; Li, D.; Cao, J.; Wang, B.; Liang, H.; Zheng, H.; Xie, Y.; Tap, J.; Lepage, P.; Bertalan, M.; Batto, J. M.; Hansen, T.; le Paslier, D.; Linneberg, A.; Nielsen, H. B.; Pelletier, E.; Renault, P.; Sicheritz-Ponten, T.; Turner, K.; Zhu, H.; Yu, C.; Li, S.; Jian, M.; Zhou, Y.; Li, Y.; Zhang, X.; Li, S.; Qin, N.; Yang, H.; Wang, J.; Brunak, S.; Doré, J.; Guarner, F.; Kristiansen, K.; Pedersen, O.; Parkhill, J.; Weissenbach, J.; Bork, P.; Ehrlich, S. D.; Wang, J. A human gut microbial gene catalogue established by metagenomic sequencing. *Nature* **2010**, *464*, 59−65.

(23) Hitch, T. C. A.; Thomas, B. J.; Friedersdorff, J. C. A.; Ougham, H.; Creevey, C. J. Deep sequence analysis reveals the ovine rumen as a reservoir of antibiotic resistance genes. *Environ. Pollut.* **2018**, *235*, 571−575.

https://doi.org/10.1021/acs.est.1c08654
Environ. Sci. Technol. XXXX, XXX, XXX−XXX

(24) Moura, A.; Soares, M.; Pereira, C.; Leitao, N.; Henriques, I.; Correia, A. INTEGRALL: a database and search engine for integrons, integrases and gene cassettes. *Bioinformatics* **2009**, *25*, 1096−1098.
(25) Siguier, P.; Gourbeyre, E.; Varani, A.; Ton-Hoang, B.; Chandler, M. Everyman's Guide to Bacterial Insertion Sequences. *Microbiol. Spectr.* **2015**, *3*, No. MDNA3-0030-2014.
(26) Kristiansson, E.; Fick, J.; Janzon, A.; Grabic, R.; Rutgersson, C.; Weijdegård, B.; Söderström, H.; Larsson, D. G. Pyrosequencing of antibiotic-contaminated river sediments reveals high levels of resistance and gene transfer elements. *PLoS One* **2011**, *6*, No. e17038.
(27) Zhou, M.; Wu, Y.; Kudinha, T.; Jia, P.; Wang, L.; Xu, Y.; Yang, Q. Comprehensive Pathogen Identification, Antibiotic Resistance, and Virulence Genes Prediction Directly From Simulated Blood Samples and Positive Blood Cultures by Nanopore Metagenomic Sequencing. *Front. Genet.* **2021**, *12*, No. 620009.
(28) Li, B.; Ju, F.; Cai, L.; Zhang, T. Profile and Fate of Bacterial Pathogens in Sewage Treatment Plants Revealed by High-Throughput Metagenomic Approach. *Environ. Sci. Technol.* **2015**, *49*, 10492−10502.
(29) Kim, Y. S.; Choi, E. J.; Lee, W. H.; Choi, S. J.; Roh, T. Y.; Park, J.; Jee, Y. K.; Zhu, Z.; Koh, Y. Y.; Gho, Y. S.; Kim, Y. K. Extracellular vesicles, especially derived from Gram-negative bacteria, in indoor dust induce neutrophilic pulmonary inflammation associated with both Th1 and Th17 cell responses. *Clin. Exp. Allergy* **2013**, *43*, 443−454.
(30) Biller, S. J.; Schubotz, F.; Roggensack, S. E.; Thompson, A. W.; Summons, R. E.; Chisholm, S. W. Bacterial vesicles in marine ecosystems. *Science* **2014**, *343*, 183−186.
(31) Biller, S. J.; McDaniel, L. D.; Breitbart, M.; Rogers, E.; Paul, J. H.; Chisholm, S. W. Membrane vesicles in sea water: heterogeneous DNA content and implications for viral abundance estimates. *ISME J.* **2017**, *11*, 394−404.
(32) Johnson, T. A.; Stedtfeld, R. D.; Wang, Q.; Cole, J. R.; Hashsham, S. A.; Looft, T.; Zhu, Y. G.; Tiedje, J. M. Clusters of Antibiotic Resistance Genes Enriched Together Stay Together in Swine Agriculture. *MBio* **2016**, *7*, e02214−e02215.
(33) Burrus, V.; Pavlovic, G.; Decaris, B.; Guédon, G. Conjugative transposons: the tip of the iceberg. *Mol. Microbiol.* **2002**, *46*, 601−610.
(34) Ding, L. J.; Zhou, X. Y.; Zhu, Y. G. Microbiome and antibiotic resistome in household dust from Beijing, China. *Environ. Int.* **2020**, *139*, No. 105702.
(35) Li, N.; Chai, Y.; Ying, G. G.; Jones, K. C.; Deng, W. J. Airborne antibiotic resistance genes in Hong Kong kindergartens. *Environ. Pollut.* **2020**, *260*, No. 114009.
(36) Schulz, E.; Karagianni, A.; Koch, M.; Fuhrmann, G. Hot EVs - How temperature affects extracellular vesicles. *Eur. J. Pharm. Biopharm.* **2020**, *146*, 55−63.
(37) Zhang, M.; Ghosh, S.; Kumar, M.; Santiana, M.; Bleck, C. K. E.; Chaimongkol, N.; Altan-Bonnet, N.; Shuai, D. Emerging Pathogenic Unit of Vesicle-Cloaked Murine Norovirus Clusters is Resistant to Environmental Stresses and UV254 Disinfection. *Environ. Sci. Technol.* **2021**, *55*, 6197−6205.
(38) Yang, D.; Chen, X.; Wang, J.; Lou, Q.; Lou, Y.; Li, L.; Wang, H.; Chen, J.; Wu, M.; Song, X.; Qian, Y. Dysregulated Lung Commensal Bacteria Drive Interleukin-17B Production to Promote Pulmonary Fibrosis through Their Outer Membrane Vesicles. *Immunity* **2019**, *50*, 692−706.e7.
(39) Deo, P.; Chow, S. H.; Han, M. L.; Speir, M.; Huang, C.; Schittenhelm, R. B.; Dhital, S.; Emery, J.; Li, J.; Kile, B. T.; Vince, J. E.; Lawlor, K. E.; Naderer, T. Mitochondrial dysfunction caused by outer membrane vesicles from Gram-negative bacteria activates intrinsic apoptosis and inflammation. *Nat. Microbiol.* **2020**, *5*, 1418−1427.
(40) Ren, D.; Walker, A. N.; Daines, D. A. Toxin-antitoxin loci vapBC-1 and vapXD contribute to survival and virulence in nontypeable Haemophilus influenzae. *BMC Microbiol.* **2012**, *12*, 263.
(41) Tulkens, J.; Vergauwen, G.; Van Deun, J.; Geeurickx, E.; Dhondt, B.; Lippens, L.; De Scheerder, M. A.; Miinalainen, I.; Rappu, P.; De Geest, B. G.; Vandecasteele, K.; Laukens, D.; Vandekerckhove, L.; Denys, H.; Vandesompele, J.; De Wever, O.; Hendrix, A. Increased levels of systemic LPS-positive bacterial extracellular vesicles in patients with intestinal barrier dysfunction. *Gut* **2020**, *69*, 191−193.
(42) Perez Vidakovics, M. L. A.; Jendholm, J.; Mörgelin, M.; Månsson, A.; Larsson, C.; Cardell, L. O.; Riesbeck, K. B cell activation by outer membrane vesicles–a novel virulence mechanism. *PLoS Pathog.* **2010**, *6*, No. e1000724.

https://doi.org/10.1021/acs.est.1c08654
Environ. Sci. Technol. XXXX, XXX, XXX−XXX